Physicochem. Probl. Miner. Process., 57(4), 2021, 168-179

http://www.journalssystem.com/ppmp

Physicochemical Problems of Mineral Processing

ISSN 1643-1049

Received February 09, 2021; reviewed; accepted June 28, 2021

On the use of Na_2SO_3 as a pyrite depressant in saline systems and the presence of kaolinite

María P. Arancibia-Bravo [1,2], Freddy A. Lucay [4], Felipe D. Sepúlveda [3] and Luis A. Cisternas [1]

[1] Departamento de Ingeniería Química y Procesos de Minerales, Universidad de Antofagasta, Chile

[2] Csiro-Chile International Center of Excellence, Las Condes, Santiago, Chile

[3] Departamento de Ingeniería en Minas, Universidad de Antofagasta, Chile

[4] Escuela de Ingeniería Química, Pontificia Universidad Católica de Valparaíso, Valparaíso, Chile

Corresponding author: arancibiabravo@gmail.com (María Pía Arancibia Bravo)

Abstract: The effect of Na_2SO_3 as a pyrite depressant in NaCl and KCl saline media and the presence of kaolinite were evaluated by zeta potential tests. Chalcopyrite was also included in the study, because pyrite usually accompanies this mineral. Subsequently, the floatability results of both minerals in the NaCl solution were optimized based on the design of experiments (DoE). The Box–Behnken DoE was applied considering the percentage of kaolinite (X_1), collector dose (X_2), and depressant dose (X_3) as factors. The results were modeled using artificial neural networks (ANNs) to construct contour plots and to determine the optimal conditions. In particular, maximization of the mass recovery of chalcopyrite and minimization of that of pyrite were sought. The particle swarm optimization algorithm was used as an optimization technique. The results indicated that the optimal conditions to maximize the floatability of chalcopyrite were kaolinite 6.85%, collector dose 3.58×10^{-3} mol/dm^3, and depressant dose 3.49×10^{-5} mol/dm^3. On the contrary, the optimal conditions to minimize the floatability of pyrite were 5% kaolinite, collector dose 5×10^{-4} mol/dm^3, and depressant dose 6.4×10^{-5} mol/dm^3. Under these conditions, the mass recoveries of chalcopyrite and pyrite were 66.1% and 14.0%, respectively. The results also indicated that the presence of kaolinite negatively affects the flotation of chalcopyrite, while the effect of Na_2SO_3 is not significant. In general, the findings suggest that Na_2SO_3 is a viable alternative to consider as a pyrite depressant in saline environments.

Keywords: Na_2SO_3, IPETC, clays; flotation, saline solution, artificial neural networks

1. Introduction

Historically, the water resource used in the flotation process comes from rivers and aquifers. In arid and semi-arid places, such as northern Chile, these resources have become scarce due to climatic and legal limitations. This has forced the use of seawater as an alternative, whether desalinated or not (Cisternas and Gálvez, 2018). The use of desalinated water has some disadvantages, such as energy consumption, waste generation, and subsequent greenhouse gas emissions during the desalination process (Herrera-León et al., 2019). Although the use of seawater without desalination does not have these disadvantages, its use is problematic due to the presence of dissolved ions (Jeldres et al., 2016). For this reason, identifying which reagents to use and in which concentrations to selectively float in media with high-ion content such as seawater is essential to avoid desalination. The use of these reagents should be considered holistically. Bulatovic and Wyslouzil (1995) indicated that depressants should be considered as important as collectors. Some reagents to depress pyrite in neutral and alkaline media are those of the oxy-sulfide type, such as sulfite (SO_3^{2-}), bisulfite (HSO_3^-), and metabisulfite ($S_2O_5^{2-}$) (Mu et al., 2016). Among them, sodium sulfite (Na_2SO_3) has been investigated as a pyrite depressant in copper sulfides (Molaei et al., 2018), enargite (Haga et al., 2012), copper depressant in minerals associated with molybdenite (Miki et al., 2018), and arsenopyrite from gold ores (Kydros K. , Angelidis T., 1993). However, these studies used fresh water for their evaluation. Such freshwater results cannot be

DOI: 10.37190/ppmp/139511

extrapolated to seawater, because freshwater does not have the same characteristics as it is composed of electrolytes such as Na^+, Cl^-, Mg^{2+}, Ca^{2+}, CO_3^{2-}, and HCO_3^-, among others (Cisternas, L., Moreno, 2014). Although the use of Na_2SO_3 has been studied, its application in saline environments has not yet been thoroughly investigated, perhaps constituting an alternative that has not yet been considered. The findings of (Zhang et al., 2020) indicated that this depressant allows working at a pH below 10, essential for processes that use seawater without desalination, as at pH over 10, there is an excessive consumption of lime.

Previous studies by the authors, when evaluating the effects of Na_2SO_3 in the presence of the collector potassium propyl xanthate (PPX), demonstrated that this depressant does not affect the floatability of chalcopyrite in saline media (Arancibia-bravo et al., 2020). The presence of clays can have an important effect in saline systems, and few studies have analyzed their presence (Jeldres et al., 2019). Uribe et al. (2017) shown that kaolinite depress chalcopyrite in seawater which may be related to formation of hydrolyzed species of calcium and magnesium. They indicated that these species can induce heterocoagulation between kaolinite and chalcopyrite (Uribe et al., 2017). However, evaluating their behavior in the presence of other minerals such as pyrite and kaolinite, using an isopropyl ethyl thionocarbamate collector (IPETC), has not been reported. This collector is currently used by mining companies that process chalcopyrite with seawater without desalination in Chile (Antofagasta Minerals). Therefore, determining whether Na_2SO_3 in the presence of IPETC in saline media affects the floatability of chalcopyrite and pyrite is a matter of interest to the industry. Traditionally, the method to evaluate the effects of a reagent in the flotation process on a laboratory scale is to analyze one variable at a time. These types of experimental designs require a large number of resources and a significant amount of time to globally evaluate a system, and may not be able to obtain the best operational conditions. Instead, response surface methodology (RSM) has become a more efficient alternative for this purpose. RSM considers all of the factors simultaneously, which allows not only to determine the effect of each factor, but also the effect of the interactions between the factors. This methodology consists of three steps. A design of experiments (DoE) must first be generated (Garud et al., 2017). There are several types of DoEs, including the Box–Behnken DoE (BBD). The BBD design measures the quadratic effects and interactions of the input factors (Box G. and Behnken D., 1960). Second, using a polynomial model (PM), a model of the RSM is generated (Carson et al., 1997). The last step is to obtain the optimal conditions based on the model (Bezerra et al., 2008). Studies have shown that PMs are easy to implement, but with low adjustments when their systems are not linear (Jin et al., 2001). Other studies have shown that it is common in multiphase systems for PMs not to deliver good results, given the nature of the behavior of these systems (Cisternas et al., 2020). Therefore, the use of ANNs has been proposed as a good alternative to PMs in mineral processing (Lucay et al., 2020). Several other works have shown that ANNs are an adequate tool for RSM (Arias et al., 2020, 2018; Xiao and Zhu, 2010; Yadav et al., 2018, 2017; Zulfiqar et al., 2019). Thus, this work aimed to study the use of Na_2SO_3 as a pyrite depressant in the presence of chalcopyrite and kaolinite in saline media of NaCl and KCl. To do this, zeta potential and microflotation studies were performed at different concentrations of Na_2SO_3 and IPETC. Subsequently, to optimize the metallurgical response, by maximizing the recovery of chalcopyrite and minimizing the recovery of pyrite, DoE and an ANN were used.

2. Materials and methods

To evaluate the effects generated by the depressant Na_2SO_3 on the recovery of chalcopyrite and pyrite in NaCl solutions, two sets of experiments were performed, one for chalcopyrite and another for pyrite. In both cases, the percentage of kaolinite (X_1), collector dose (X_2), and depressant dose (X_3) were considered as input factors. Once the results were obtained, ANN training was carried out using a hybrid algorithm to predict the optimal conditions for the recovery of chalcopyrite. For the generation of DoE and RSM, Minitab 18 software was used. To optimize the recovery of chalcopyrite and pyrite, a radial basis function neural network (RBFNN) was used, implemented in R Studio software, following the methodology proposed by Lucay et al. (2020).

2.1. Experimental procedure

A pure mineral of chalcopyrite (from Durango, Mexico) and pyrite (from Huanzala, Peru) purchased through Ward Science, as well as pure kaolinite provided by Merk, were used. A mechanical size

reduction was made for rock sizes exceeding 20 mm. Subsequently, a manual size reduction was carried out, using agate mortar. Then, the minerals were classified in meshes as having particles of between +100 and –635 Ty (+150 +20 μm). These minerals were characterized by mineralogical analysis using a Hitachi SU 5000 model scanning electron microscope and a Bruker advance d8 model X-ray diffractor. High purity (>99%) IPETC and Na_2SO_3 samples were used for the microflotation provided by Mathiesen and Merk, respectively. Particle sizes between –100 and +200 # Ty (–150 +75 μm) were used. The samples were stored in a neutral nitrogen atmosphere to prevent oxidation of the mineral. Na_2SO_3 solutions were prepared daily with deionized water of a resistivity of 18.2 MΩ cm^{-1}. Exploratory microflotation tests were conducted at a pH between 8.0 and 8.2. Collector and depressant doses in the chalcopyrite and pyrite samples, separately, between 0 and 0.02 mol/dm^3 IPETC and 0 and 0.01 mol/dm^3 Na_2SO_3 in concentrations of 6.4 mol/dm^3 and 0.1 mol/dm^3, respectively, were used to determine the minimum and maximum doses and to subsequently apply the DoE. Microflotation tests were performed in duplicate in a 150 cm^3 modified Hallimond tube (Farrokhrouz and Haghi, 2009) with 1 g of total mineral, reporting averages. The NaCl or KCl solution was conditioned to pH 8.0–8.2 using NaOH and HCl. Subsequently, the mineral was added, and the pH was adjusted. Finally, the collector was added, and it was conditioned for 15 min at 900 r/min. In the case of using both the collector and the depressant in the test, the collector was first added and conditioned for 5 min, and then the depressant for the remaining 10 min. The samples were delicately deposited in the cell and shaken at 700 r/min. Aeration for all microflotation tests was at a nitrogen flow of 30 cm^3/min, and they floated for 1 min. The float and tail samples were filtered and dried at a maximum of 105 °C for 12 h to be massed separately. The ratio of float material to total mass fed was used for the ore recovery calculation. The floating mass ratio (R) was calculated from:

$$\text{Recovery} = m_1 / (m_1 + m_2) \times 100\% \quad (1)$$

where m_1 and m_2 are the masses of the floating and non-floating fractions, respectively. For the three cases and the microflotations generated by BBD, 1 g of chalcopyrite mineral was used.

The zeta potential measurement was carried out in samples of chalcopyrite, pyrite, and pure kaolinite with particle sizes of –635 # Ty (–20 μm), to measure the electrostatic repulsion/attraction of the particles (Shehata and Nasr-El-Din, 2015). For this, Zetameter 4.0 model equipment was used, and solutions at 0.01 mol/dm^3 NaCl and KCl were prepared for the study. These saline concentrations were used so as not to affect the reading of the equipment due to the excess of ions present (Uribe, 2017). A hundred milligrams of the mineral was used with 50 cm^3 of the solution previously conditioned to the required pH. Each sample was conditioned for 15 min, as suggested by Fullston et al. (1999), to achieve equilibrium of the reactions in the system in the measurements of the zeta potential. The samples were shaken at 700 r/min in the absence and presence of IPETC and Na_2SO_3 according to the case studied. Ten readings were made for each assay in a pH range of 3–12.

2.2. Mathematical modeling

2.2.1. Response surface methodology using the Box–Behnken design (BBD)

The experimental evaluation was carried out through applying optimization by RSM using BBD. The estimation of the tests to be carried out was determined by applying the following equation:

$$N = 2k(k - 1) + C_0 \quad (2)$$

where N is the number of trials, k is the number of factors to combine, and C0 refers to the central points. For cases 1 and 2, three factors (k = 3) and three central points (C_0 = 3) were combined. These combinations gave a total of 15 trials.

2.2.2. Artificial neural networks (ANNs)

ANNs are based on the behavior and function of the human brain, and they are capable of learning and solving a wide range of complex problems. Forward neural networks (FNNs) are a special type of ANN. An FNN allows perceiving a computational model in the form of a structure/network (Ojha, Abraham, and Snásel, 2017). Among the FNNs, the multilayer perceptron and the radial-basis function neural network (RBFNN) stand out because they have been used in many practical applications. Mathematically, the network output is calculated as:

$$y_i = \sum_{j=1}^{h} w_j^i \varphi_j(x) \quad (3)$$

where $i = 1, .., q$, $j = 1, .., h$, q is the number of outputs from the network, h is the number of neurons in the hidden layer, w_j^i are the weights, and $\varphi_j(x)$ is the activation function of the neurons. The activation function used in this work was the Gaussian radial-based function:

$$\varphi_j(x) = exp\left(-\frac{\|x-c_j\|_2^{\ 2}}{2\sigma_j^2}\right) \quad (4)$$

RBFNN coefficients w_j^i, c_j, and σ_j ^ were determined using a hybrid algorithm, that is, a combination of the differential evolution algorithm and the backpropagation algorithm. This combination of algorithms helps to ensure the effectiveness of the global search of the metaheuristic algorithm (i.e., the differential evolution algorithm) and the effectiveness of the local search of the conventional algorithm (i.e., the backpropagation algorithm). The hybrid algorithm was fully programmed in the Rstudio environment, and the DoParallel package was used to improve its performance.

3. Results and discussion

3.1. Mineralogical characterization of the samples

The results of the SEM and XRD analyses of the samples indicate that the chalcopyrite was comprised of 34.4% Fe, 31.39% Cu, and 31.02% S, while the remainder was impurities of Si, Ca, and Mg. The pyrite comprised 49.79% S and 50.21% Fe, while the kaolinite was formed of 44.53% Al, 48.57% Si, 4.44% Ti, and 2.47% Fe. This characterization indicates that all of the samples had high purity (>98%) and did not show oxidation on their surfaces. The SEM and XRD analyses of each sample are presented in Fig. 1.

Table 1. Chemical composition of the chalcopyrite, pyrite, and kaolinite samples (wt%)

Sample	Cu	Fe	S	Ca	Si	Mg	Al	Si	Ti
Chalcopyrite	31.39	34.40	31.02	0.82	1.25	1.11	-	-	-
Pyrite	-	50.21	49.79	-	-	-	-	-	-
Kaolinite	-	2.47	-	-	-	-	44.53	48.57	4.44

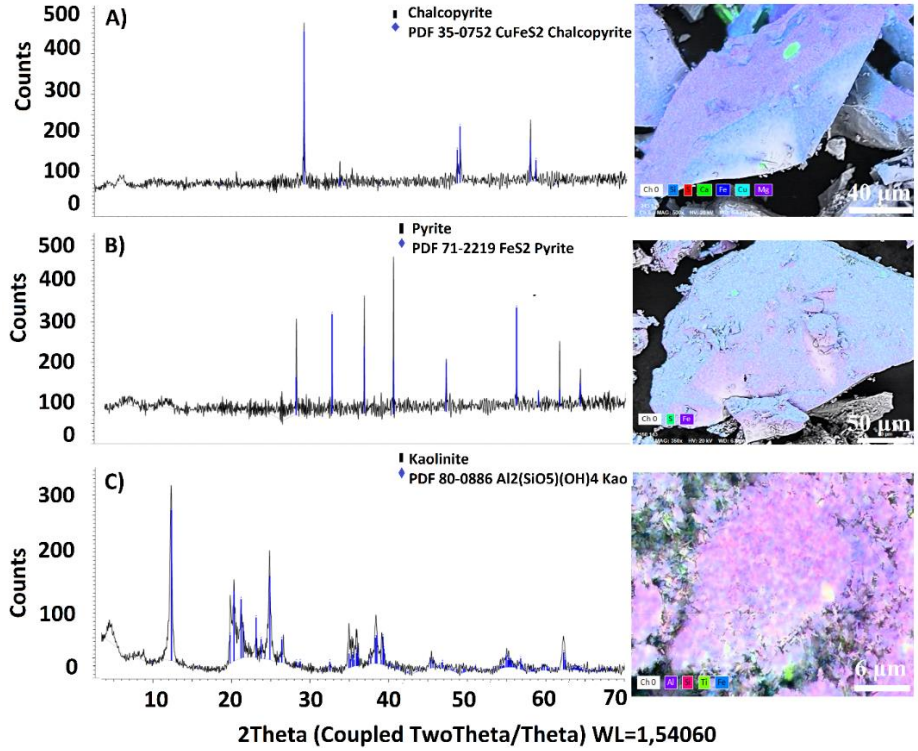

Fig. 1. XRD (left) and SEM (right) analyses of: (A) Chalcopyrite, (B) pyrite, and (C) kaolinite. The meaning of the different colors of the SEM photographs: White, oxygen; blue, silicon; red, sulfur; green, calcium; navy blue, iron; light blue, copper; magenta, magnesium

3.2. Chalcopyrite, pyrite, and kaolinite zeta potentials in the NaCl and KCl solutions

The effect of the collector and depressant on the mineral samples in the NaCl and KCl solutions was evaluated. The results are presented in Figs. 2 and 3 for the chalcopyrite, pyrite, and kaolinite minerals. For chalcopyrite, in the absence of the collector and depressant, the effects of the type of solution were similar with mean values of –20 mV. The similar potentials of chalcopyrite in both solutions replicate the findings obtained by Li et al. (2017) in their study of the effects of chlorides and by Arancibia-Bravo et al. (2020). The impact of IPETC on the surface of the chalcopyrite and in both types of solutions was negative over the entire pH range. For pyrite, IPETC generated isoelectric points (IEPs) at an acidic pH (low pH = 4.5) in the KCl solution. For NaCl, IEPs occurred at pH values lower than 6. Negative potentials above pH 5 were achieved in both solutions. Similar results were reported by Paredes et al. (2019) in the pyrite. Pyrite is known to become hydrophobic when not oxidized; therefore, to avoid IPETC adsorption on pyrite, an alkaline pH should be utilized (Leppinen, 1988). For this reason, pH 8 was selected for the experiments. For the kaolinite in NaCl, the potentials were negative throughout the studied pH range. In the case of the KCl solution, an IEP was generated at pH 6 and negative potentials at values higher than that pH. For these study conditions, the values obtained replicate those reported by Ma et al. (2012) in their study of the role of the water structure in kaolinite (Ma et al., 2012). This is attributable to the difference in ions. KCl contains K^+ ions capable of breaking the water structure and reducing the potential values of kaolinite. This facilitates the adsorption of IPETC on the mineral surface, together with the catalytic effect of clay, as suggested by Fu et al. (2020) in their IPETC study on catalytic ozonation. In NaCl, the hydrated layer that forms the Na^+ ions was higher, producing lower hydrophobicity. For the working pH (pH 8) and throughout the range of doses studied, the potentials were negative, meaning that the kaolinite remained in colloidal suspension in the flotation system.

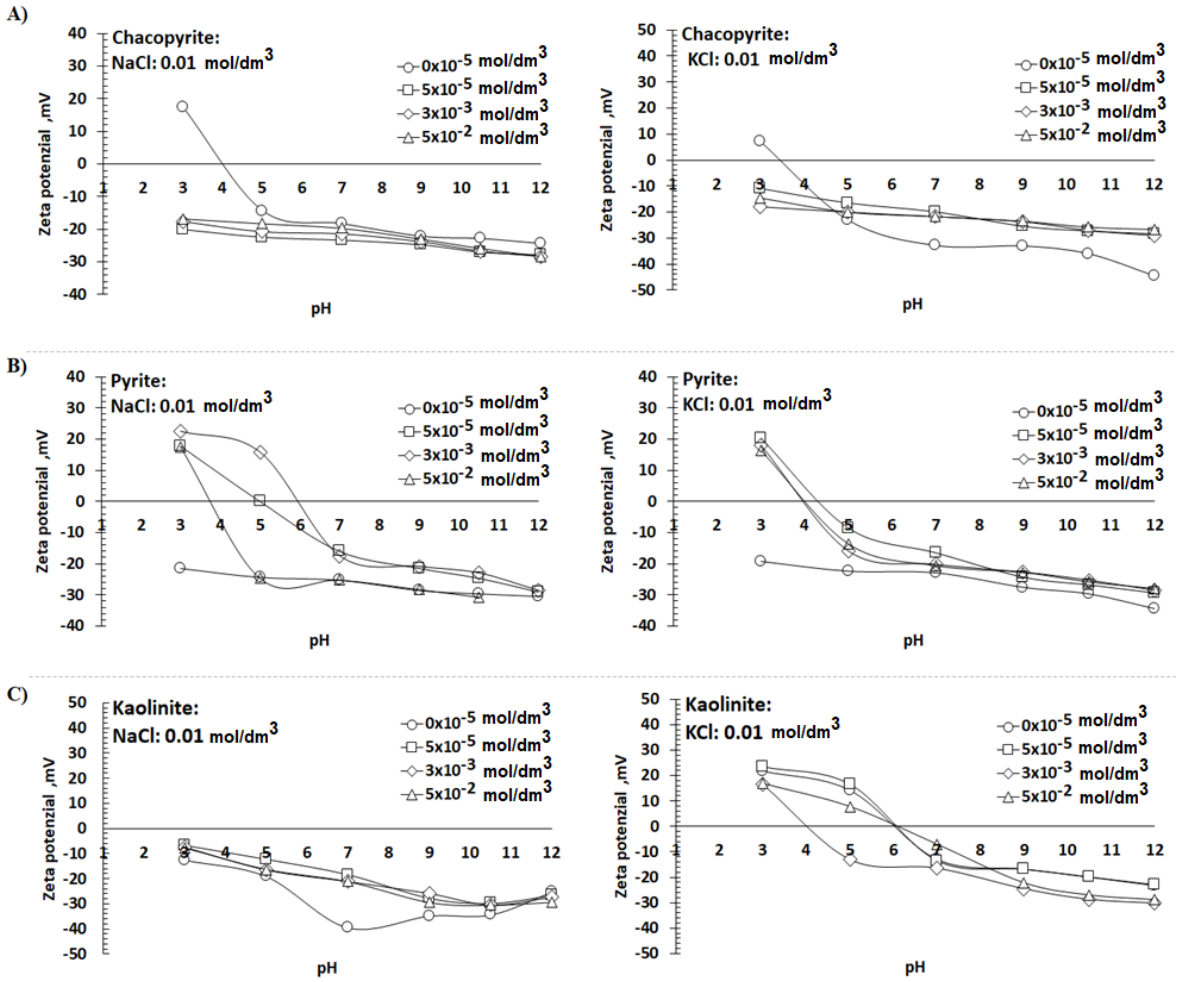

Fig. 2. Zeta potential effect of the isopropyl ethyl thionocarbamate collector (IPETC) for (A) chalcopyrite, (B) pyrite, and (C) kaolinite in the NaCl and KCl solutions. Mineral size = 20 μm; NaCl and KCl concentrations 0.01 mol/dm^3; pH = 8.0–8.2

The effects of Na_2SO_3 in the mineral samples studied in both saline solutions are presented. In the case of chalcopyrite, an IEP was achieved in the KCl solution for pH 4.5 with medium concentration e doses of Na_2SO_3. Values slightly lower than those achieved with the IPETC averaging –15 mV were generated in both solutions and for all doses at a pH greater than 7. This allowed us to deduce that Na_2SO_3 does not superficially affect chalcopyrite in alkaline pH in the absence of a collector in the system. For pyrite, Na_2SO_3 at lower values of pH 4 for KCl and pH 6 for NaCl achieved IEPs. The Na_2SO_3 must modify the surface of the mineral to increase its hydrophilicity. The mechanism is through the action of the sulfite ion (SO_3^{-2}), which consumes oxygen and turns into sulfate (SO_4^{-2}). The SO_4^{-2} interacts with the ferric/hydroxide ions present on the surface of pyrite. These interactions form layers of ferric hydroxide that make pyrite hydrophilic when it is not activated (Fuerstenau and Sabackyab, 1981). At working pH, in both solutions and across the entire dose range studied, Na_2SO_3 averaged potential values of –20 mV. In the case of kaolinite, the potentials showed changes in the IEPs for both solutions at pH 4. For the working pH, the potentials were –10 and –20 mV for KCl and NaCl, respectively. The saline solutions and the change in pH generated compression of the electrical double layer, resulting in the inversion of the potential. The effect of Na_2SO_3 on clay should not be considered harmful. As explained above, Na_2SO_3 changes from a sulfite ion into a sulfate ion. This increases the presence of OH^- in the system. The hydroxides basify the system and, added to the negative charge of the kaolinite at the working pH, suggest a repulsion of the system.

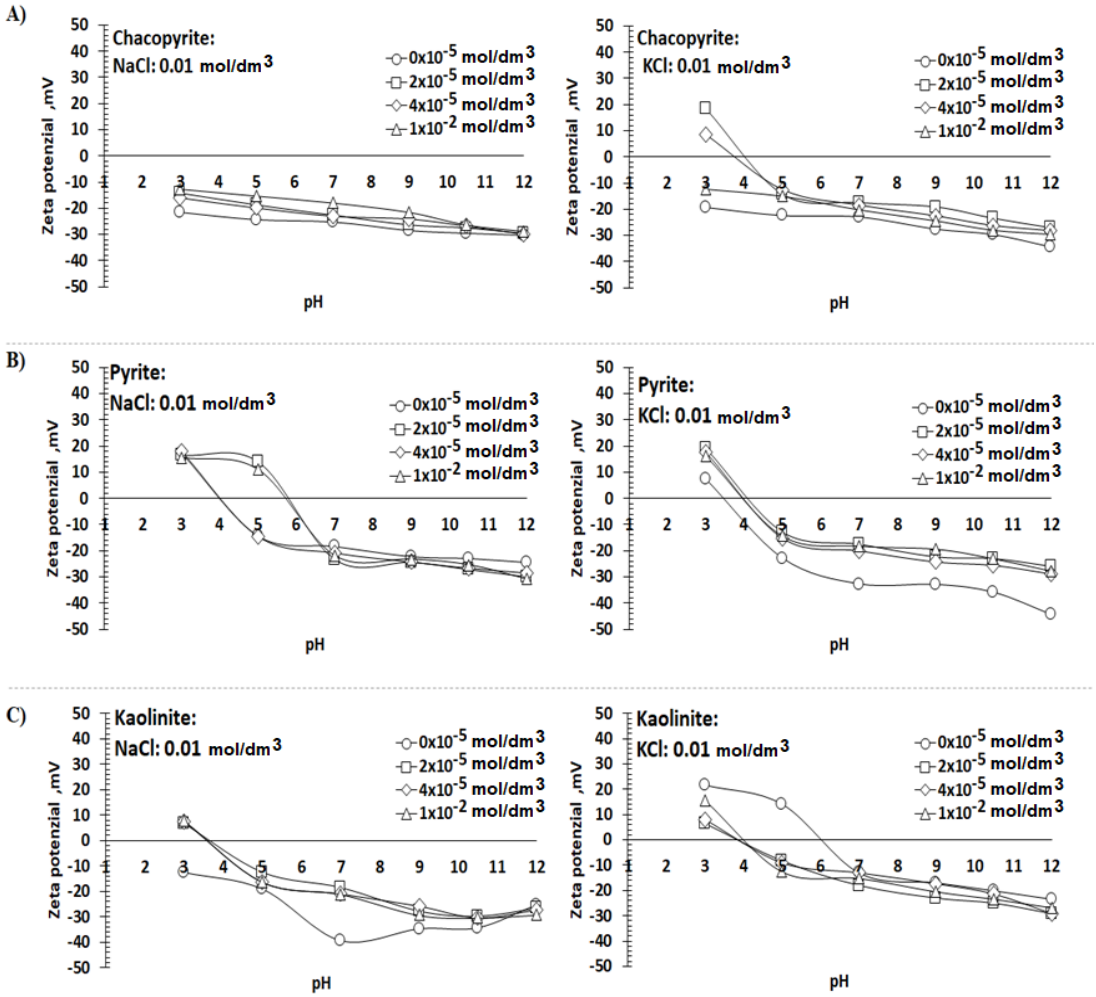

Fig. 3. Zeta potential effect of Na_2SO_3 for (A) chalcopyrite, (B) pyrite, and (C) kaolinite in the NaCl and KCl solutions. Mineral size = 20 µm; NaCl and KCl concentration= 0.01 mol/dm^3; pH = 8.0–8.2

3.3. Effects of IPETC and Na_2SO_3 on the floatability of chalcopyrite and pyrite in the NaCl and KCl solutions

In this section, the results of the preliminary microflotation tests on the chalcopyrite and pyrite minerals using IPETC and Na_2SO_3 in the NaCl and KCl solutions are shown. These tests made it possible to

determine the minimum and maximum limits of the collector and depressor to be used later in the DoE. Fig. 4A shows the recoveries after applying IPETC, and Fig. 4B after applying Na_2SO_3. The effects of IPECT on chalcopyrite showed maximum recoveries of 70% and 90% for the NaCl and KCl solutions, respectively. The recoveries increased as the concentration of the collector increased until a maximum value; after this value, the recoveries remained at a constant value. For a dose of 5×10^{-3} mol/dm^3 of IPETC, the maximums were achieved in both solutions without major changes at higher doses. The pyrite, in both solutions, obtained maximum recoveries that did not exceed 30%. This behavior is attributable to the way it was adsorbed on the mineral surface. Fairthorne et al. (1996), in their work on IPETC solutions, indicated that the form of adhesion is through chemisorption by S and O bonds on the surface of the Cu of chalcopyrite (Fairthorne et al., 1996). Leppinen et al. (1988) determined that the IPETC adhesion order in sulfur minerals is as follows: Chalcocite > chalcopyrite > pyrite. In the case of IPETC in the NaCl and KCl solutions, the trend reported by Leppinen et al. (1988) was maintained, being preferential for chalcopyrite over pyrite.

The effects of Na_2SO_3 in the chalcopyrite without the presence of a collector showed maximum recoveries of 20%. This effect is attributed to the interaction of Na_2SO_3 in active iron sites and its reducing effect, as suggested by Miki et al. (2018) in their study of chalcopyrite and molybdenite minerals. The chalcopyrite, in the presence of the depressant shown in Fig. 4B, had an oscillating behavior not seen in the pyrite. The sulfite ions, in the presence of the monovalent ions (Na^+ and K^+) of the saline solution and the divalent ion (Ca^{2+}) present on the surface of the chalcopyrite (see Table 1), explain the behavior of the mineral. The above results are attributable to variations in the oxidation–reduction reactions, as reported by the authors in their previous work (Arancibia-Bravo et al., 2020). In the pyrite, Na_2SO_3 strongly depressed throughout the range studied and in both solutions, with recoveries that did not exceed 15%. The reducing effect of Na_2SO_3 in alkaline media, such as those used in this study, promotes the generation of iron oxyhydroxide (FeO) on the surface of pyrite. This reduces the hydrophobicity of pyrite (López Valdivieso A., 2005). The depressant effect of Na_2SO_3 was achieved in low doses (1×10^{-5} mol/dm^3), with a slight reduction as the dose increased.

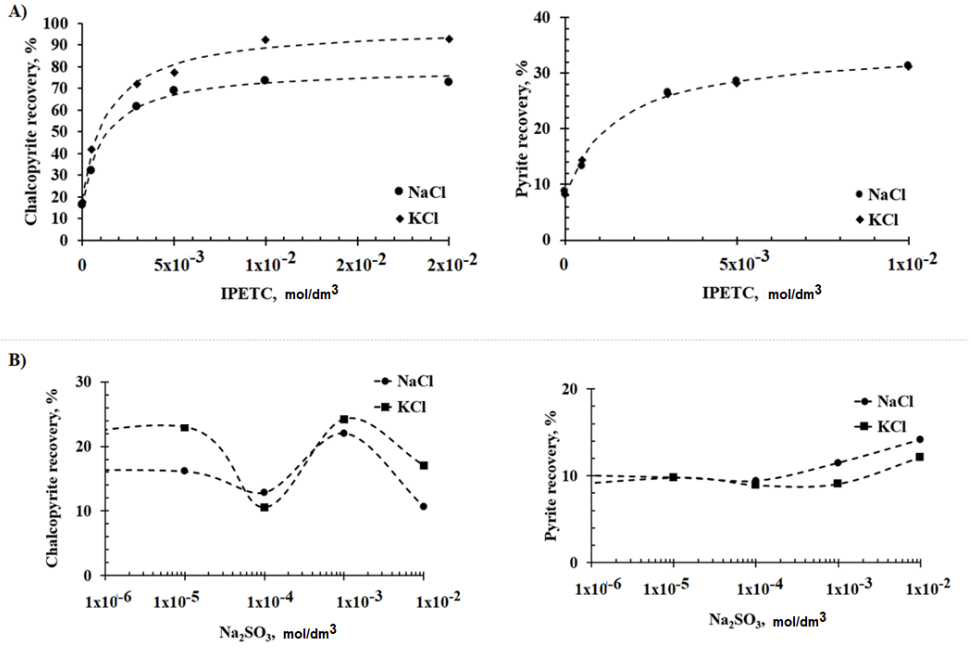

Fig. 4. Mass recovery of the chalcopyrite (left) and the pyrite (right) with (A) IPETC and (B) Na_2SO_3 in the NaCl and KCl solutions. Mineral size = 150 µm; NaCl and KCl concentrations = 0.01 mol/dm^3; pH = 8.0–8.2

These analyses allowed to determine the ranges to use in the DoE. The NaCl and KCl solutions generated minimal differences in the flotation of the chalcopyrite and pyrite when analyzed independently in the presence of the depressant. It is for this reason that, to determine the ranges to be used in the DoE, the NaCl solution was used. The results indicated that the minimum and maximum doses of IPETC were between 5×10^{-4} and 5×10^{-3} mol/dm^3. In the case of Na_2SO_3,, it depressed both minerals when applied without the presence of a collector at very low doses. Thus, the minimum and

maximum ranges considered for the Na_2SO_3 concentration in the DoE were between 1.6×10^{-5} and 6.4×10^{-5} mol/dm^3.

3.4. Effect of Na_2SO_3 on chalcopyrite and pyrite with a high kaolinite content

The previous results allowed to determine the collector and depressor doses able to guarantee the floatability of the mineral with minimum doses of the reagents. To determine the effects of the depressant, the NaCl solution was used, as it was the one with the lowest mass recovery and because it was the salt with the highest presence in seawater (>78%) (Castro and Laskowski, 2011). This criterion was used to avoid influencing the mineral floatability of the results and to effectively determine the sensitivity of the system. In these case studies, the variable percentage of kaolinite was added to evaluate the performance of Na_2SO_3. The clays present in saline systems were recovered by dragging in the flotation, thereby reducing the quality of the concentrate. This is the cause of the stability of the foam, presenting smaller bubble sizes by inhibiting coalescence in saline solutions (Liu and Peng, 2014)(Arancibia-bravo et al., 2019). Kaolinite is a clay of common occurrence in copper sulfide mining deposits. Therefore, controlling the amount kaolinite that enters the process is important. This is why high percentages of kaolinite were considered in this study, in order to see its effects on the system. Table 2 summarizes the minimum, average, and maximum levels considered for the generation of the DoE.

Table 1. The factors and their levels used for the Box–Behnken design of experiments (BBD) experiment

Factors	Coded variable level		
	Low	Center	High
	–1	0	+1
X_1: Kaolinite, %	5	15	25
X_2: IPETC, mol/dm^3	5.0×10^{-4}	2.8×10^{-3}	5.0×10^{-3}
X_3: Na_2SO_3, mol/dm^3	1.6×10^{-5}	4.0×10^{-5}	6.4×10^{-5}

As already known, the DoE generates combinations that are characterized by not repeating one another. The exception is the central points that serve to determine the variability of the experimental errors. In these cases, these points gave a standard deviation of $\sigma = 0.301$ and $\sigma = 0.276$ for the chalcopyrite and pyrite, respectively.

Fig. 5 shows the RSM generated by the ANN when trained with the results obtained from applying the DoE to both minerals. It presents the contours generated for the chalcopyrite (left) and the pyrite (right). In these graphs, the kaolinite concentration (X_1) was kept fixed at 5%, 15%, and 25%, and the collector (X_2) and depressant (X_3) were varied. The graphs allow to see the areas where higher or lower recoveries were achieved depending on the values of the collector and depressant concentrations. For the chalcopyrite, maximum recoveries of 65.7% were obtained at maximum IPETC dose (5.0×10^{-3} mol/dm^3). An increase in the dose of Na_2SO_3 affected the recovery of the chalcopyrite in the presence of the minimum and maximum values of IPETC. The above was explained by Miki et al. (2018), who determined that increasing the dose of Na_2SO_3 reduces the hydrophobicity of pure chalcopyrite. At its midpoint, further recovery can be achieved. The results indicate that Na_2SO_3 does not greatly affect the floatability of chalcopyrite at low doses.

Clays in NaCl solutions tend to form aggregates with one another due to the presence of Na^+ ions. Ma et al. (2012) determined that this type of ion reduces the zeta potential (see Fig. 3C), promoting the floatability of kaolinite. The above can be attributed to the reduction in the floatability of chalcopyrite due to the mechanical dragging of kaolinite in the system, affecting the quality of the concentrate. In the case of the pyrite, average doses of IPETC (2.8×10^{-3} mol/dm^3) generated higher recoveries in the presence of kaolinite. In the case of Na_2SO_3, it was a negative effect on the entire dose range studied. This indicates that ANNs should find a zone optimized at medium-to-high collector doses and minimum depressant doses for chalcopyrite. In the case of the pyrite, with minimum doses of Na_2SO_3 (1.6×10^{-5} mol/dm^3) and medium–high doses of IPETC (2.8×10^{-3} to 5.0×10^{-3} mol/dm^3), it was possible to minimize the recovery of the mineral. Table 3 shows the results of the runs of the DoE generated by the BBD for both minerals.

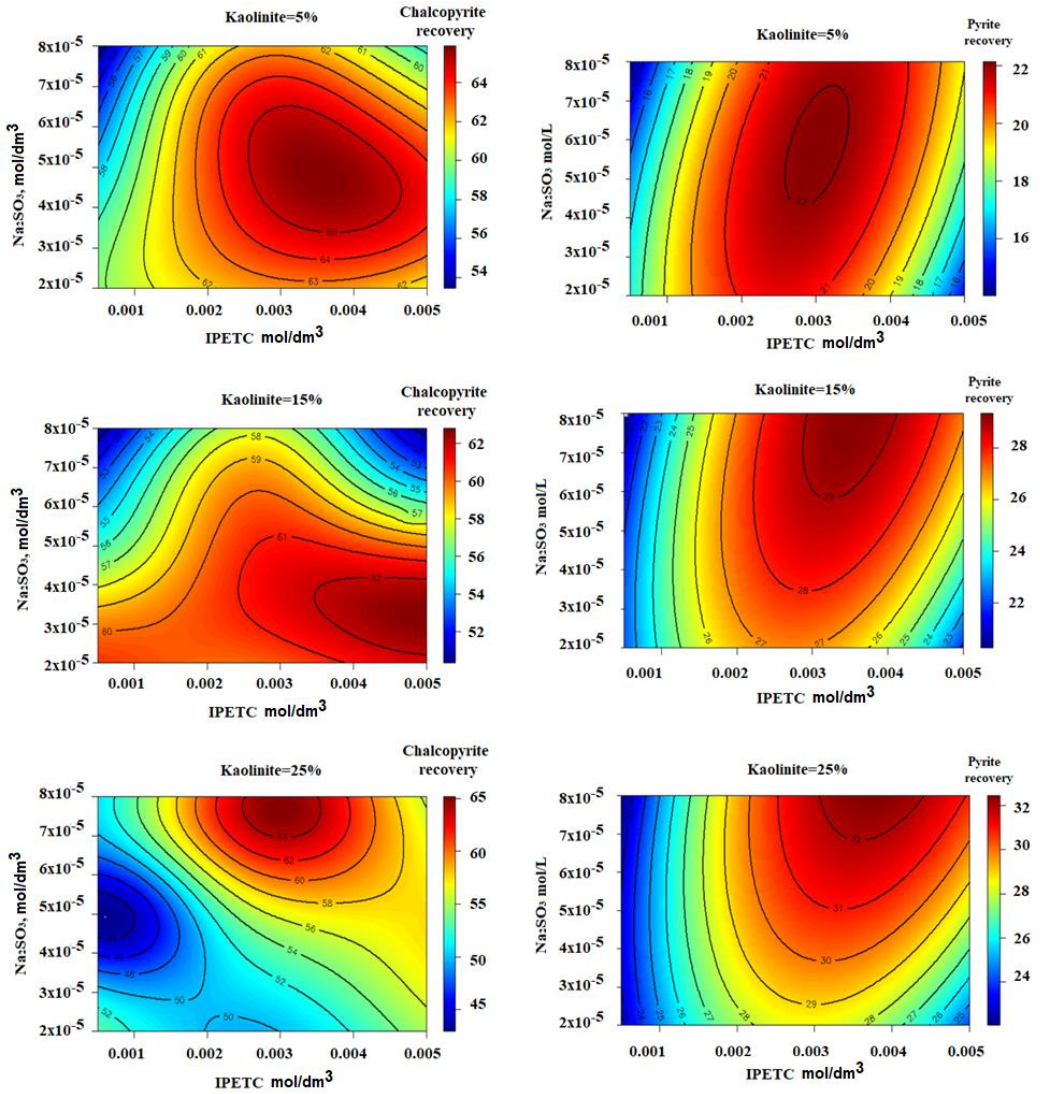

Fig. 5. Effect of Na_2SO_3 and contour surface recovery of the chalcopyrite (left) and the pyrite (right) using an artificial neural network (ANN) (R Studio). Mineral size = 150 μm; NaCl concentrations= 0.01 mol/dm³; pH = 8.0

Table 2. Microflotation recoveries for the chalcopyrite and pyrite with the BBD

Test	Kaolinite %	IPETC mol/dm³	Na_2SO_3 mol/dm³	Recovery %	
	X_1	X_2	X_3	Chalcopyrite	Pyrite
1	–1	0	1	63.7	20.8
2	0	0	0	63.8	28.4
3	0	1	1	49.5	27.5
4	1	0	–1	49.0	29.2
5	–1	0	–1	64.4	20.0
6	–1	–1	0	58.8	17.9
7	1	0	1	65.0	32.7
8	0	0	0	63.2	28.5
9	–1	1	0	65.7	18.2
10	0	1	–1	62.3	22.6
11	1	1	0	56.7	26.7
12	0	–1	1	48.9	19.5
13	0	0	0	63.4	28.9
14	1	–1	0	43.2	22.6
15	0	–1	–1	61.2	22.0

The flotation process was defined via the following continuous optimization problem to determine the optimal conditions: $maximize/minimize\ f(x)$, $s.a.\ g(x) \leq 0$, where $f(x)$ represents an ANN, and $g(x)$ represents the process of operational constraints. To solve the problem, particle swarm optimization, included in evolutionary computation (Kachitvichyanukul, 2012), was implemented. Particle swarm optimization implements a population of particles, a so-called "swarm," where each particle updates its position according to a defined scheme. If some particles violate the constraints of the defined optimization problem, then its objective function value is penalized. Table 4 shows the results obtained when optimizing the factors using the ANN. The fit values were 96.1% for the trained data. For the chalcopyrite, values close to the minimum kaolinite value and close to the medium collector and depressor values were necessary to maximize the mineral's recovery. For the pyrite, the ANN suggested a minimum doses of kaolinite and the collector and a maximum dose of the depressant to minimize the floatability of the mineral. With these doses, the recovery of the chalcopyrite was 66.08% and 14.01%. In both cases, kaolinite should be operated in minimum ranges to avoid losses in mineral recovery.

Table 3. Optimized values obtained using the ANN

Factor	Chalcopyrite	Pyrite
X_1: Kaolinite, %	6.8	5
X_2: IPETC, mol/dm^3	3.6×10^{-3}	5.0×10^{-4}
X_3: Na_2SO_3, mol/dm^3	3.5×10^{-5}	6.4×10^{-5}
Recovery, %	66.1	14.01

4. Conclusions

In the case of pyrite recovery, the NaCl and KCl solutions did not generate significant differences, averaging recoveries of 30% in the absence of the collector. For chalcopyrite recovery, the KCl solution generated greater floatability of >90% versus 70% in NaCl when evaluating the IPETC collector. The optimization by RSM reported harmful effects of kaolinite on the flotation in both minerals, whereas Na_2SO_3 did not generate a critical impact on chalcopyrite recovery. To minimize the effect of clay, the operation should be conducted at minimum kaolinite ranges, medium collector doses, and maximum depressant rates for both minerals. Finally, these results indicate that sodium sulfite is a viable alternative to consider as a pyrite depressant in saline media, but further in depth research is necessary in seawater without desalination.

Acknowledgments

The authors thank the financial support from INNOVA CORFO Projects Csiro Chile, 10CEII-9007. Special thanks to Renato Acosta-Flores and Unidad de Equipamiento Científico (MAINI) Universidad Católica del Norte for the SEM and XRD analyses. The authors are grateful for the support of the ANID through research grant Fondecyt 1180826. Special thanks to Laboratorio Soluciones Analíticas (LSA) Universidad Católica del Norte for the shared infrastructure for the microflotation development. Special thanks to Mr. Fabrizio Colombo and the Mathiesen (Chile) mining team for providing samples of the flotation reagents. Finally, thanks to students Robert Clavel and Felipe Pino for their help in the experimental development.

References

ARANCIBIA-BRAVO, M.P., LOPEZ-VALDIVIESO, A., CISTERNAS, L.A., 2020. *Effects of Potassium Propyl Xanthate Collector and Sodium Sulfite Depressant on the Floatability of Chalcopyrite in Seawater and KCl Solutions*. Minerals. https://doi.org/10.3390/min10110991

ARANCIBIA-BRAVO, M.P., LUCAY, F.A., LÓPEZ, J., CISTERNAS, L.A., 2019. *Modeling the effect of air flow , impeller speed , frother dosages , and salt concentrations on the bubbles size using response surface methodology*. Minerals Engineering 132, 142–148.

ARIAS, D., RIVAS, M., GUIÑEZ, R., CISTERNAS, L.A., 2018. *Modeling the calcium and magnesium removal from seawater by immobilized biomass of ureolytic bacteria bacillus subtilis through response surface methodology and artificial neural networks*. Desalination and Water Treatment 118, 294–303.

ARIAS, D., VILLCA, G., PÁNICO, A., CISTERNAS, L.A., JELDRES, R.I., GONZÁLEZ-BENITO, G., RIVAS, M., 2020. *Partial desalination of seawater for mining processes through a fluidized bed bioreactor filled with immobilized cells of Bacillus subtilis LN8B*. Desalination 482, 114388.

BEZERRA, M.A., SANTELLI, R.E., OLIVEIRA, E.P., VILLAR, L.S., ESCALEIRA, L.A., 2008. *Response surface methodology (RSM) as a tool for optimization in analytical chemistry*. Talanta 76, 965–77.

BOX G. AND BEHNKEN D., 1960. *Technometrics Some New Three Level Designs for the Study of Quantitative Variables Some New Three Level Designs for the Study of Quantitative Variables*. Technometrics 455–475.

BULATOVIC, S., WYSLOUZIL, D.M., 1995. *Selection and evaluation of different depressants systems for flotation of complex sulphide ores*. Minerals Engineering 8, 63–76.

CASTRO, S., LASKOWSKI, J.S., 2011. *Froth flotation in saline water*. KONA Powder and Particle Journal 29, 4–15.

CISTERNAS, L., MORENO, L., 2014. *Seawater in Mining: Fundamentals and Applications (in Spanish)*. Master Ril, Santiago, Chile.

CISTERNAS, L.A., GÁLVEZ, E.D., 2018. T*he use of seawater in mining*. Mineral Processing and Extractive Metallurgy Review 39.

CISTERNAS, L.A., LUCAY, F.A., BOTERO, Y.L., 2020. *Trends in modeling, design, and optimization of multiphase systems in minerals processing*. Minerals. https://doi.org/10.3390/min10010022

FAIRTHORNE, G., FORNASIERO, D., RALSTON, J., 1996. *Solution properties of thionocarbamate collectors*. 46, 137–153.

FARROKHROUZ, M., HAGHI, H., 2009. *The application of Hallimond tube for floatability study of pure Galena.* 13th Conference on Environment and Mineral Processing 89–96. https://doi.org/10.13140/2.1.2825.6969

FU, P., LIN, X., WANG, L., MA, Y., 2020. *Applied Clay Science Catalytic ozonation of refractory O -isopropyl- N - ethylthionocarbamate collector with coexisted kaolinite in sulfide flotation wastewaters*. Applied Clay Science 198, 105834.

FUERSTENAU M. AND SABACKYAB B., 1981. *On the natural floatability of sulfides*. International journal of minerals processing 8, 79–84.

FULLSTON, D., FORNASIERO, D., RALSTON, J., 1999. *Zeta potential study of the oxidation of copper sulfide minerals*. Colloids and Surfaces A: Physicochemical and Engineering Aspects 146, 113–121.

GARUD, S.S., KARIMI, I.A., KRAFT, M., 2017. *Design of computer experiments: A review.* Computers and Chemical Engineering 106, 71–95.

HAGA, K., TONGAMP, W., SHIBAYAMA, A., 2012. *Investigation of Flotation Parameters for Copper Recovery from Enargite and Chalcopyrite Mixed Ore*. Materials Transactions 53, 707–715.

HERRERA-LEÓN, S., CRUZ, C., KRASLAWSKI, A., CISTERNAS, L.A., 2019. *Current situation and major challenges of desalination in Chile*. Desalination and water treatment 171, 93–104.

JELDRES, R.I., FORBES, L., CISTERNAS, L.A., 2016. *Effect of Seawater on Sulfide Ore Flotation: A Review*. Mineral Processing and Extractive Metallurgy Review 37, 369–384.

JELDRES, R.I., URIBE, L., CISTERNAS, L.A., GUTIERREZ, L., LEIVA, W.H., VALENZUELA, J., 2019. *The effect of clay minerals on the process of flotation of copper ores - A critical review*. Applied Clay Science 170.

JIN, R., CHEN, W., SIMPSON, T.W., 2001. *Comparative studies of metamodelling techniques under multiple modelling criteria.* Struct Multidisc Optim 1–13.

KACHITVICHYANUKUL, V., 2012. *Comparison of Three Evolutionary Algorithms : GA, PSO, and DE*. Industrial Engineering and Management Systems 11, 215–223.

KYDROS K. , ANGELIDIS T., . MATIS K., 1993. *Selective flotation of an auriferous bulk pyrite arsenopyrite concentrate in presence of sodium sulphoxy - salts*. Minerals Engineering 6, 1257–1264.

LEPPINEN J.O., 1988. *FTIR Study of Thionocarbamate Adsorption on Sulfide Minerals*. Colloids and Surfaces 32, 113–125.

LI, Y., LI, W., XIAO, Q., HE, N., REN, Z., LARTEY, C., GERSON, A., 2017. *The Influence of Common Monovalent and Divalent Chlorides on Chalcopyrite Flotation*. Minerals 7, 111.

LIU, D., PENG, Y., 2014. *Reducing the entrainment of clay minerals in flotation using tap and saline water*. Powder Technology 253, 216–222.

LÓPEZ VALDIVIESO A., 2005. *Flotación de calcopirita , pirita y molibdenita en minerales de cobre tipo pórfidos*, in: X Simposio Sobre Procesamiento de Minerales. Chillan, Chile, pp. 1–29.

LUCAY, F.A., SALES-CRUZ, M., GÁLVEZ, E.D., CISTERNAS, 2020. *Modeling of the Complex Behavior through an Improved Response Surface Methodology Modeling of the Complex Behavior through an Improved Response Surface Methodology*. Mineral Processing and Extractive Metallurgy Review 00, 1–27.

MA, M., BRUCKARD, W.J., MCCALLUM, D., 2012. *Role of Water Structure-Making / Breaking Ions in the Cationic Flotation of Kaolinite : Implications for Iron Ore Processing*. International Journal of Mining Engineering and Mineral Processing 1, 17–20.

MIKI, H., HIRAJIMA, T., MUTA, Y., SUYANTARA, G.P.W., SASAKI, K., 2018. *Effect of sodium sulfite on floatability of chalcopyrite and molybdenite*. Minerals 8. https://doi.org/10.3390/min8040172

MOLAEI, N., HOSEINIAN, F.S., REZAI, B., 2018. *A study on the effect of active pyrite on flotation of porphyry copper ores.* Physicochemical Problems of Mineral Processing 54, 922–933.

MU, Y., PENG, Y., LAUTEN, R.A., 2016. *The depression of pyrite in selective flotation by different reagent systems – A Literature review*. Minerals Engineering 96–97, 143–156.

OJHA, V.K., ABRAHAM, A., SNÁSEL, V., 2017. *Metaheuristic Design of Feedforward Neural Networks: A Review of Two Decades of Research*. Engineering Applications of Artificial Intelligence 60, 97–116.

PAREDES A., ACUÑA S., GUTIERREZ L., T.P., 2019. Zeta Potential of Pyrite Particles in Concentrated Solutions of Monovalent Seawater Electrolytes and Amyl Xanthate. Minerals. https://doi.org/10.3390/min9100584

SHEHATA, A.M., NASR-EL-DIN, H.A., 2015. *Zeta Potential Measurements: Impact of Salinity on Sandstone Minerals* 13–15. SPE International Symposium on Oilfield Chemistry, The Woodlands, Texas, USA https://doi.org/10.2118/173763-ms

URIBE, L., GUTIERREZ, L., LASKOWSKI, J.S., CASTRO, S., 2017. *Role of calcium and magnesium cations in the interactions between kaolinite and chalcopyrite in seawater*. Physicochemical Problems of Mineral Processing 53, 737-749.

URIBE, L.M., 2017. *Efecto del agua de mar en la recuperación de minerales de cobre-molibdeno por procesos de flotación*. Universidad de Concepción. Concepción, Chile.

XIAO, G., ZHU, Z., 2010. *Friction materials development by using DOE/RSM and artificial neural network*. Tribology International 43, 218–227.

YADAV, A.M., CHAURASIA, R.C., SURESH, N., GAJBHIYE, P., 2018. *Application of artificial neural networks and response surface methodology approaches for the prediction of oil agglomeration process*. Fuel 220, 826–836.

YADAV, A.M., NIKKAM, S., GAJBHIYE, P., TYEB, M.H., 2017. *Modeling and optimization of coal oil agglomeration using response surface methodology and artificial neural network approaches*. International Journal of Mineral Processing 163, 55–63.

ZHANG, Y., LIU, R., SUN, W., WANG, L., DONG, Y., WANG, C., 2020. *Electrochemical mechanism and flotation of chalcopyrite and galena in the presence of sodium silicate and sodium sulfite*. Transactions of Nonferrous Metals Society of China 30, 1091–1101.

ZULFIQAR, M., FAKHRUL, M., SAMSUDIN, R., SUFIAN, S., 2019. *Chemistry Modelling and optimization of photocatalytic degradation of phenol via TiO2 nanoparticles : An insight into response surface methodology and artificial neural network.* Journal of Photochemistry & Photobiology, A: Chemistry 384, 112039.